

Modelling Virchow's Triad to Improve Stroke Risk Assessment in Atrial Fibrillation Patients

Ahmed Qureshi¹, Maximilian Balmus¹, Steven E Williams^{1,2}, Gregory Y H Lip³,
David A Nordsletten^{1,4}, Oleg Aslanidi¹, Adelaide de Vecchi¹

¹School of Biomedical Engineering and Imaging Sciences, King's College London, United Kingdom

²Deanery of Clinical Sciences, University of Edinburgh, United Kingdom

³Liverpool Heart and Chest Hospital, University of Liverpool, United Kingdom

⁴Department of Biomedical Engineering, University of Michigan, USA

Abstract

Atrial fibrillation (AF) is associated with a significantly increased risk of stroke due to the presence of three pro-thrombotic mechanisms known as Virchow's triad – blood stasis, endothelial damage and hypercoagulability – which primarily occur in the left atrial appendage (LAA). In-silico evaluation of each factor can improve upon the current empirical stroke risk stratification for AF patients.

*Computational fluid dynamics simulations were performed on two patient-specific models of the left atrium, one in sinus rhythm (SR) and one in AF to quantify blood stasis and metrics of endothelial damage. Hypercoagulability was assessed by solving reaction-diffusion-convection equations for thrombin, fibrinogen and fibrin – three key clotting proteins, and varying initial concentrations of fibrinogen in accordance with clinical literature. An original grading system is proposed (**A** = low, **B** = moderate, **C** = high risk) for each component of the triad to form a patient-specific risk profile.*

*The SR patient had a risk profile of [**A**, **B**, **A**] showing a low-moderate risk of thrombus formation, while the AF patient had [**C**, **B**, **C**], indicating a very high risk of thrombus formation and increased potential for stroke.*

This novel modelling approach encapsulates all fundamental mechanisms of thrombus formation and may be used to improve stroke risk assessment for AF patients.

1. Introduction

Atrial fibrillation (AF) is a widespread cardiac arrhythmia linked to one third of all thromboembolic strokes [1]. AF significantly increases the risk of stroke by localised activation of three pro-thrombotic mechanisms – blood stasis, hypercoagulability and endothelial damage – known as Virchow's triad [2]. A pro-thrombotic state is primarily achieved in the left atrial appendage (LAA), an extension to the left atrium (LA) reported to harbour >90% of AF-related thrombi.

Pathological thrombus formation in AF patients occurs

when the cardiac endothelial lining is damaged, triggering a cascade of biochemical reactions mediated by the catalytic conversion of plasma fibrinogen to an insoluble fibrin thrombus by the enzyme thrombin.

Current stroke risk stratification schemes, such as the CHA₂DS₂-VASc score, are limited by relying on patient comorbidities (e.g., age, sex) rather than the mechanisms underlying thrombus formation (Virchow's triad), leading to challenges in decision-making for some patient cohorts.

Cardiac imaging tools, such as spontaneous echo contrast, can identify thrombi after their formation, but remain unable to predict patients at risk of AF-related stroke, owing a need for innovative, *in-silico* approaches to stratify patient risks. State-of-the-art modelling methods can identify some aspects of the triad, yet a comprehensive evaluation remains to be addressed [3].

We propose a novel modelling pipeline that leverages cardiac imaging data for mechanistic quantification of all aspects of Virchow's triad to evaluate patient thrombogenicity.

2. Methods

Each component of Virchow's triad was modelled by finite-element simulations in *CHeart* [4]. LA models were generated from temporally varying Cine MRI data from two patients [5]. An original grading system is proposed to assess patient-specific risks of thrombus formation based on clinically defined parameters.

2.1 Blood Stasis

Computational fluid dynamics (CFD) simulations were performed to quantify blood stasis over 10 cardiac cycles. 3D tetrahedral volume models (~1 million elements) were generated by manual segmentation and meshing of the LA. Myocardial deformation was prescribed by image-derived wall motion tracking. The resulting deforming meshes reproduced patient-specific contractility, one during an episode of AF and one during regular sinus rhythm (SR).

The Navier-Stokes equations were solved in the Arbitrary-Eulerian-Lagrangian frame of reference to account for domain deformation. Blood density was set to $\rho = 1060 \text{ Kg/m}^3$ and viscosity to $\mu = 3.5 \times 10^{-3} \text{ Pa.s}$. Mitral valve (MV) flow velocities were computed from the left ventricular volumetric flow rate and prescribed on the MV annulus to drive LA flow in through the pulmonary veins (PVs) (Fig. 1) [3].

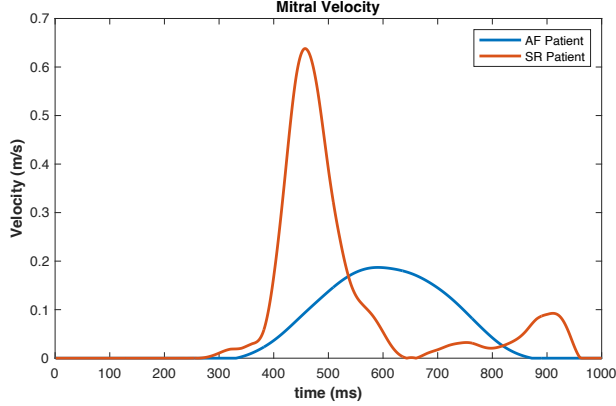


Figure 1: MV velocity profiles for patient in AF (blue) and SR (red).

2.2 Endothelial Damage

Regions prone to thrombogenesis can be determined by the endothelial cell activation potential (ECAP), calculated by the ratio of the oscillatory shear index (OSI) to the time averaged wall shear stress (TAWSS), shown in Eq. 1 [6]. High ECAP values indicate large oscillatory shear flows and low wall shear stresses (τ_w) and were selected as locations to initiate thrombus formation in the subsequent coagulation simulations.

$$ECAP = \frac{OSI}{TAWSS} = \frac{\frac{1}{2} \left(1 - \frac{\left| \int_0^T \tau_w dt \right|}{\int_0^T |\tau_w| dt} \right)}{\frac{1}{T} \int_0^T |\tau_w| dt} \quad (1)$$

2.3 Hypercoagulability

Blood velocity values, \mathbf{u} , calculated from the CFD simulations in Section 2.1, were coupled with a system of reaction-diffusion-convection equations for the key coagulation proteins; thrombin (Th), fibrinogen (Fg) and fibrin (Fn), to model thrombus growth dynamics (2 - 4).

$$\frac{\partial Th}{\partial t} = D_{Th} \Delta Th - \mathbf{u} \cdot \nabla Th + R_{Th} \quad (2)$$

$$\frac{\partial Fg}{\partial t} = D_{Fg} \Delta Fg - \mathbf{u} \cdot \nabla Fg - K_{eff} Fg Th \quad (3)$$

$$\frac{\partial Fn}{\partial t} = D_{Fn} \Delta Fn - \mathbf{u} \cdot \nabla Fn + K_{eff} Fg Th \quad (4)$$

Diffusion coefficients, constants and rates of reaction were taken from our previous work [7]. The initial concentration of plasma fibrinogen was set to 2.5 g/L in SR and 4.0 g/L in AF to represent the hypercoagulable state in AF, as described in clinical literature [8].

2.4 Quantifying Thrombogenic Risk

Grading of thrombogenicity for each aspect of the triad was defined on a risk scale from **A** (low), **B** (moderate) to **C** (high) to derive a patient-specific mechanistic risk profile, with values summarised in Table 1.

Table 1. Values from literature and simulations used to grade risk of thrombus formation in the LAA. Peak blood velocities in the LAA (\mathbf{u}_{max}) [9], maximum ECAP and remnant fibrin concentration after 10 cardiac cycles (Fn) were used to categorise thrombogenic risk.

	\mathbf{u}_{max} (m/s)	Max. ECAP	Fn (mmol/m ³)
A	> 0.5	< 2	< 0.5
B	0.2 - 0.5	2 - 4	0.5 - 3
C	< 0.2	> 4	> 3

3. Results

3.1 Blood Stasis

SR: A rapid increase in blood flow velocities was observed after 300 ms throughout the LA. After 10 cardiac cycles, blood flow velocities in the LA cavity ranged from 0-2.2 m/s with a mean of 0.28 m/s. The highest velocities were at the PVs and in vortices which formed in the LA.

Velocities in the LAA had a mean of 0.12 m/s and a peak \mathbf{u}_{max} of 0.78 m/s that was detected in a vortex entering halfway into the LAA of the SR patient (Fig 2a). Beyond this vortex, blood velocity dropped sharply to 0.12 m/s near the tip of the LAA shown by dark blue/black streamlines in Fig 2a.

AF: LA velocities were 69% lower on average throughout the cardiac cycle with a mean of 0.087 m/s and maximum of 0.36 m/s. Fewer vortices formed in the LA during AF but were larger in size and slower (0.23 m/s).

Velocities in the LAA were low throughout the 10 cardiac cycles with a mean velocity of 0.02 m/s and \mathbf{u}_{max} of 0.19 m/s. A small vortical structure can be seen near the lower entrance of the LAA (Fig 2d) where the peak velocity was achieved. Dark blue/black streamlines depict the low velocities seen throughout the LAA in Fig 2d.

3.2 Endothelial Damage

SR: LAA ECAP values ranged from 0.9-2.7 with a mean of 1.4. A small region of high ECAP can be seen in

the upper LAA entrance (Fig 2b) with a value of 2.7.

AF: ECAP values were higher in AF with an average of 2.0 and more regions with ECAP > 3. Multiple areas with peak values of 3.5 were found in the AF LAA (Fig 2e).

3.3. Hypercoagulability

SR: During the first cardiac cycle, the fibrin concentration rose to 1.1 mmol/m^3 at the site of initial injury after 200 ms. This quickly decreased after each LA contraction as the vortex (Fig 2a) washed fibrin away to low concentrations of 0.1 mmol/m^3 after 2 cardiac cycles and $1e^{-3} \text{ mmol/m}^3$ after 4 cardiac cycles (Fig 2c).

AF: After the first 4 cardiac cycles the fibrin thrombus reached 3.5 mmol/m^3 , as low flow velocities in the LAA facilitated uninterrupted growth (Fig 2f). After the 5th cardiac cycle, the thrombus detached from the site of injury and was carried by the low advective velocity towards the tip of the LAA where it circulated till the 10th cycle (Fig.

3). Dissipation of the thrombus as it moved in the blood stream reduced the final fibrin concentration to 3.2 mmol/m^3 .

3.4 Patient Risk Profiles

Table 2. Categorisation of risk for each component of Virchow's triad for the SR and AF patients.

	Blood stasis (u_{max} , m/s)	Endothelial damage (max. ECAP)	Hyper-coagulability (Fn, mmol/m^3)
SR	0.78 → A	2.7 → B	$2e^{-6}$ → A
AF	0.19 → C	3.5 → B	3.2 → C

Giving final risk profiles of **[A, B, A]** for SR, with a low to moderate risk of thrombus formation and **[C, B, C]** for the AF patient, with a very high risk of thrombus formation and stroke.

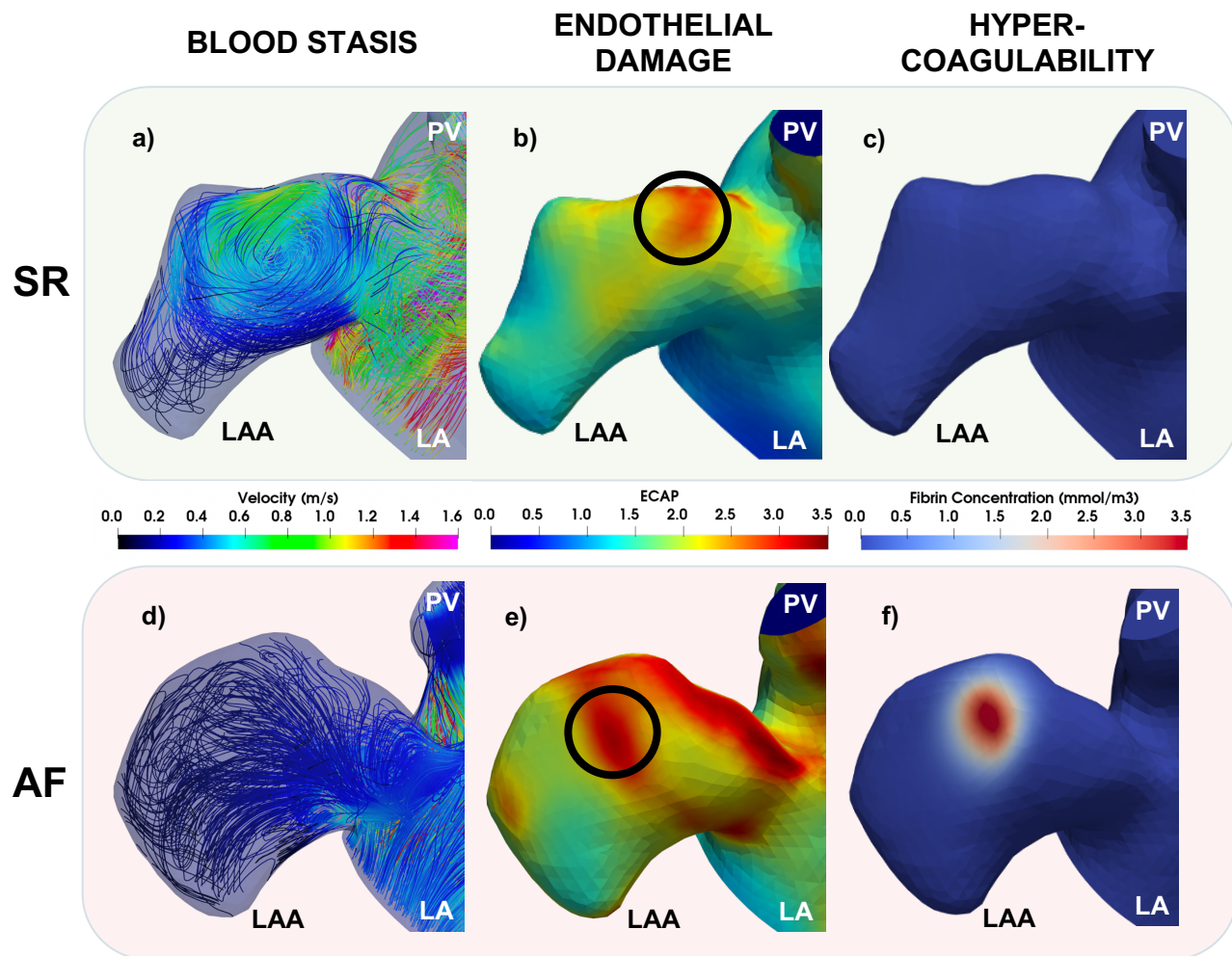


Figure 2. Modelling each aspect of Virchow's triad in the LAA during SR (top row) and AF (bottom row). Peak LAA blood flow velocities (a, d), ECAP with the location of the maximum ECAP chosen to initiate coagulation (b, e and black circles) and fibrin thrombus growth due to coagulation after 4 cardiac cycles shown (c, f).

4. Discussion

This study presents the first comprehensive evaluation of all aspects of Virchow's triad and proposes a novel mechanistic approach to quantify and improve stroke risk assessment on a patient-specific basis.

The two patient cases explored in this study demonstrate the clear difference in thrombogenicity between SR and AF (Table 2). The SR patient's risk profile of [A, B, A] had a moderate risk linked to endothelial damage which was outweighed by low blood stasis (> 0.5 m/s) and healthy plasma fibrinogen levels, which may indicate that presence of one factor in Virchow's triad alone may not be sufficient for pathological thrombus formation.

The very high-risk profile of [C, B, C] in the AF patient illustrated the effect of all aspects of Virchow's triad being activated. Low blood flow velocities of less than 0.2 m/s in the LAA promoted thrombus formation by enhanced thrombotic protein generation and reduced washout. Furthermore, the increased fibrinogen concentration (4 g/L) to induce a hypercoagulable state provided more substrate for fibrin production. This simulation resulted in thrombus growth and detachment in the LAA which matches the physiology preceding thromboembolic stroke, as seen in Fig. 3.

These results are consistent with the episodic nature of AF, in which patients can suddenly switch from AF, where low flow velocities facilitate thrombus growth, to SR where the formed thrombus may be ejected from the LA towards the brain causing stroke.

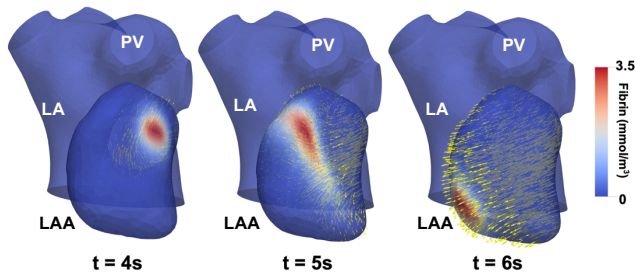


Figure 3. Detachment of fibrin thrombus from initial site of injury and movement in the bloodstream to the tip of the LAA in the AF patient.

5. Conclusion

This modelling pipeline shows promise in its ability to run patient-specific simulations, quantify risk, and predict occurrence of stroke. The development of *in-silico* tools for the evaluation of patient thrombogenicity as described in this study can help to understand the complex mechanistic processes which influence thrombus formation in AF. The proposed novel risk profiling system can enable clinicians to have a more accurate and mechanistic assessment of patient stroke risks.

Acknowledgments

This research was supported by the EPSRC [EP/R513064/1].

References

- [1] B. Freedman, T. S. Potpara, and G. Y. H. Lip, "Stroke prevention in atrial fibrillation," *The Lancet*, vol. 388, no. 10046, pp. 806–817, Aug. 2016
- [2] W. Y. Ding, D. Gupta, and G. Lip, "Atrial fibrillation and the prothrombotic state: revisiting Virchow's triad in 2020," *Heart*, p. heartjnl-2020-316977, 2020
- [3] D. Dillon-Murphy *et al.*, "Modeling left atrial flow, energy, blood heating distribution in response to catheter ablation therapy," *Frontiers in Physiology*, vol. 9, p. 1757, Dec. 2018
- [4] J. Lee *et al.*, "Multiphysics computational modeling in CHeart," *SIAM Journal on Scientific Computing*, vol. 38, no. 3, pp. C150–C178, 2016
- [5] A. Qureshi *et al.*, "Modelling left atrial flow and blood coagulation for risk of thrombus formation in atrial fibrillation," in *2020 Computing in Cardiology Conference (CinC)*, Dec. 2020, vol. 47.
- [6] P. di Achille, G. Tellides, C. A. Figueroa, and J. D. Humphrey, "A haemodynamic predictor of intraluminal thrombus formation in abdominal aortic aneurysms," *Proceedings of the Royal Society A: Mathematical, Physical and Engineering Sciences*, vol. 470, no. 2172, p. 20140163, Dec. 2014
- [7] A. Qureshi *et al.*, "Left atrial appendage morphology impacts thrombus formation risks in multi-physics atrial models," in *2021 Computing in Cardiology (CinC)*, Sep. 2021, pp. 1–4.
- [8] G. Y. H. Lip, G. D. O. Lowe, A. Rumley, and F. G. Dunn, "Increased markers of thrombogenesis in chronic atrial fibrillation: effects of warfarin treatment.," *Heart*, vol. 73, no. 6, pp. 527–533, Jun. 1995
- [9] M. Handke, A. Harloff, A. Hetzel, M. Olschewski, C. Bode, and A. Geibel, "Left atrial appendage flow velocity as a quantitative surrogate parameter for thromboembolic risk" *Journal of the American Society of Echocardiography*, vol. 18, no. 12, pp. 1366–1372, Dec. 2005,

Address for correspondence:

Ahmed Qureshi; School of Biomedical Engineering and Imaging Sciences, King's College London, 3rd Floor Lambeth Wing, St Thomas' Hospital, London, SE1 7EH, UK;
E-mail: ahmed.qureshi@kcl.ac.uk